



Production and Characterization of Activated Carbon from Oil-palm Shell for Carboxylic Acid Adsorption

HECTOR RUIZ¹, MONICA ZAMBTRANO¹, LILIANA GIRALDO²,
ROCIO SIERRA¹ and JUAN CARLOS MORENO-PIRAJAN^{3*}

¹Departamento de Ingeniería Química – Universidad de los Andes,
Cra. 1 Este 19A-40 – CEP: 111711 – Bogotá D. C. - BOG – Colombia

²Departamento de Química – Universidad Nacional de Colombia,
Cra. 30 No 43-00-CEP: 111711 – Bogotá D. C. - BOG – Colombia

³Facultad de Ciencias, Departamento de Química – Universidad de los Andes,
Grupo de Investigación en Sólidos Porosos y Calorimetría, Cra. 1 Este 19A-40 – CEP: 111711 –
Bogotá D. C. - BOG – Colombia

*Corresponding author E-mail: jumoreno@uniandes.edu.co

<http://dx.doi.org/10.13005/ojc/310217>

(Received: September 11, 2014; Accepted: October 10, 2014)

ABSTRACT

In this study, the recovery of volatile carboxylic acids (VCA) by adsorption onto activated carbon adsorbent (CA) was explored. The CA was synthesized from palm-oil kernel shells using H_3PO_4 at 10 and 60% w/w as activating agent. The samples produced in this manner were labeled as CA10A, CA60A respectively. Also KOH was used as activating agent at 10 and 60% w/w. In this case, the produced samples were labeled as CA10B, CA60B respectively. After activation, the surface of all four CA samples was extensively characterized both physically and chemically. The obtained CA adsorption behavior for VCA was assessed by submerging samples of CA in solutions at a fixed initial VCA concentration. Because some of the acids were adsorbed on the CA surface, the VCA concentration in solution was reduced. Carbon CA60B exhibited the greatest adsorption capacity, reaching 1300 mg of adsorbed acids/g carbon. Five adsorption isotherms models were fitted to experimental data. The Langmuir-Freundlich model described best the adsorption phenomena. Desorption behavior was assessed by placing CA after adsorption in water and was not high, which forces to reconsider either de desorption mechanism proposed in this study and/ or the use CA as synthesized here for VCA recovery.

Keywords: carboxylic acids; activated carbon; oil-palm kernel shell; equilibrium isotherms.

INTRODUCTION

Economic and population growth increase energy demands. Nowadays, an important fraction

of the energy consumed worldwide is obtained from fossil fuel resources, which are highly pollutant. In Colombia, fossil fuels are mixed with first generation ethanol or biodiesel (methyl esters), both

derived from monocultures (sugarcane and oil palm respectively), thereby promoting deforestation¹. To decrease these negative environmental impacts, second generation fuels are increasingly considered. The MixAlco® process (Figure 1)[2], is a biorefining technology developed to obtain chemical products of high commercial value (e.g., acetic acid, ketones, esters and alcohols) and fuels from digestible waste. The process comprises a fermentation step from which a mixture of VCA is obtained and neutralized to the corresponding carboxylic salts, which are then separated by evaporation or amine absorption and submitted to chemical downstream processing². The concentration of salts in the fermentation broth has been measured as high as 30 g/L at the laboratory level^{3,4}, averaging 20 g/L. Higher salts concentrations may be inhibitory for fermentation.

The adsorption of the acids produced during fermentation has been proposed as an alternative to evaporation. This alternative is advantageous because; (1) No salts neutralization would be required, saving resources and allowing for high acids production during fermentation (2) The high economic and energetic costs of evaporation may be greatly diminished. In this study, the use of activated carbon synthesized from low costs and high available lignocellulosic waste (oil-palm shell) [4,5] is assessed as adsorbent of volatile carboxylic acids.

METHODS AND EXPERIMENTAL

Preparation of adsorbents

Oil palm-shell was provided and collected from an oil-extraction plant in the town of Puerto Rico located in Meta - Colombia. The original sample contained palm shells as well as nut residues, which were manually separated. The nut free shells were washed multiple times with distilled water to eliminate dirt and fibers. Washed shells were distributed over shallow aluminum trays and placed in an oven at 74°C for four days to eliminate free moisture. Dry shells were grinded in a knife mill and sieved afterwards, using Tyler meshes 4 (4.75 mm), 8 (2.38 mm) and 12 (1.68 mm). The fraction used as substrate for CA synthesis was -4/+12 (between 2-5 and 4.75 mm particle size), corresponding to more than 90% of the material.

Chemical Impregnation

The chemical impregnation was carried out using two phosphoric acid solutions (10 and 60% w/w) and two potassium hydroxide solutions (10 and 60% w/w). Oil-palm shells were impregnated in the aforementioned solutions, using an impregnation ratio of 1:2 (1 volume of shell per 2 volumes of solution). For impregnation the solid-liquid mixture was shaken for 1h, left to impregnate for 24 h and then placed in an oven at 74°C for three days in order to completely dry the sample.

Carbonization and sample labeling

Carbonization of impregnated palm shells was carried out in a tube furnace under a high purity nitrogen flow of 80 mL/min at a heating flow rate of 5°C/min until a temperature of 800°C was reached. The obtained solids were thoroughly washed with distilled water in a Soxhlet extractor in order to eliminate acid or base remaining on the solids surface and then dried in a furnace at 74°C. The obtained material after drying was denominated activated carbon adsorbent (CA). Each sample was labeled according to the agent used for activation (A for Acid, B for alkaline) and its concentration (10 and 60%) such that for example sample CA60B was carbon impregnated with KOH at 60%.

Characterization of the activated carbons and precursor

For the physical and chemical characterization of each of the CA produced (CA10A, CA60A, CA10B and CA60B), the following tests were performed:

Nitrogen adsorption isotherms

Isotherms were measured in an Autosorb IQ2 porous solids analysis equipment. Prior to these measurements, the samples were degasified at 250°C for two hours. Surface area was estimated through the Brunauer-Emmett-Teller (BET) model, pore volume through the Dubinin-Radushkevich (DR) model and pore distribution through Density Functional Theory (DFT) model.

DTA

The four different samples of CA, were submitted Thermogravimetric Analysis (TGA) and Differential Thermal Analysis of thermal treatment in an inert environment (obtained through a constant flow of N₂) using a STA 449 F3 Jupiter Simultaneous

TGA-DSC Netzsch (Germany) between 25°C to 900 °C, using a heating rate of 10°C/min.

Fourier transform infrared spectroscopy (FT-IR)

FT-IR was performed using a Nicolet™iS™10 FT-IR Spectrometer (Thermo Scientific, USA) for all four CA and for the raw material to study the surface functional groups.

Boehm titration

Boehm method was used to quantify surface functional groups of the carbon by titration. It starts by placing 0.25 g of CA samples in 4 falcon tubes. To each of these tubes, 25 mL of the following 0.1 M solutions were added respectively: sodium hydroxide (NaOH), sodium carbonate (Na₂CO₃), sodium bicarbonate (NaHCO₃) and hydrochloric acid (HCl). The tubes were sealed and shaken for 5 days at room temperature. Samples were then filtered and 5 mL of the filtrates were titrated with an acid (HCl, 0.1 M) or base (NaOH, 0.1M) with 0.05 mL increments using an automatic CG840B Schott titrator⁶.

Point of zero charge (PZC)

The existence of surface functional groups cause both negatively and positively charged surface sites in aqueous solution, depending on the pH. The PZC is the required pH to obtain a net superficial charge equal to zero (pH_{PZC}). At pH_{PZC} < pH, the carbon surface becomes negatively charged, which is favorable for the adsorption of cationic substances. On the contrary, at pH_{PZC} > pH the carbon surface becomes positively charged and the adsorption of anionic substances will be favored. In order to modify the nature and concentration of surface functional groups, thermal or chemical post-treatments can be used. To determine the PZC, ten different carbon masses were taken from the four CA. Each one of the samples was placed in a falcon tube and 25 mL of 0.1 M sodium chloride solution (NaCl) was added. Samples were shaken for 2 days at a constant temperature. The pH of each resulting solution was measured.

Adsorption procedure

For the adsorption experiments a stock solution with 13.85 g/L acetic acid, 0.67 g/L propionic acid and 4.95 g/L butyric acid was prepared. During adsorption experiments, several

weights of CA between 0 and 0.55 g were introduced in Schott containers. To each of the containers with CA samples, 25 mL of stock solution were added. The solid-liquid mixture was shaken for 24 h at 30°C. The quantity of adsorbed acids expressed as the adsorbent phase concentration was calculated according to the following equation:

$$\mu_c = \frac{V(C_0 - C_e)}{m} \quad \dots(1)$$

where μ_c is the adsorbent phase concentration in milligrams of acid adsorbed per gram of adsorbent (mg/g), C_0 and C_e are the initial concentration and equilibrium concentrations (mg/L), V is the volume of solution, and m is the mass of adsorbent.

Equilibrium adsorption isotherms

Ten solutions of VCA were prepared with different acid concentrations by diluting a stock solution prepared as discussed in Section 2.5 using a dilution factor up to 20. These solutions were placed in Schott containers and 0.1 g of activated carbon were added. The solutions were placed in a shaker at 30°C for 24 h. The procedure was repeated at 40°C.

Desorption

The activated carbons after adsorption were filtered and placed in a tray dryer for 2 h without heating. The dry carbons were placed in Schott containers with 25 mL of water. The containers were placed in a shaker at 40°C for 24 h, after which a liquid sample was taken for analysis.

Gas chromatography (GC) analysis

All samples for GC analysis were mixed with internal standard (valeric acid, 3.53 g/L) [3]. 1 mL of sample was placed in a vial and acidified with phosphoric acid 85% (w/w). Samples were analyzed by gas chromatography using a FID detector in order to measure the final concentration of acetic, propionic and butyric acid in each sample.

RESULTS

Physical characteristics of CA

The nitrogen isotherms for CA10A, CA60A, CA10B and CA60B are shown in Figure 2.

For all carbons, the nitrogen isotherms were found to be of Type I (IUPAC classification) regardless the activating agent (H_3PO_4 or KOH) used during CA synthesis. Type I isotherms are characterized by microporous solids having relatively small external surfaces, the uptake limit being governed by the accessible micropore volume rather than by the internal surface area^{7,8}. Pore distribution for all CA is shown in Figure 3. Both micropores (less than 2 nm) and mesopores (between 2 and 50 nm) are observed in all samples. For samples CA10A and CA60A pore sizes were observed within a range from 1 to 4.2 nm, while for samples CA10B and CA60B pore sizes were within the range from 0.96 to 5 nm.

The nitrogen isotherms allow for the calculation of surface area, total volume of pores, and average diameter (Table 1). Carbons CA10B and CA60B exhibited the greatest superficial area and pore volumes. These parameters were at least twice the superficial area and pore volume observed for CA60A, the sample with the least superficial area and pore volume; thus, the activating agent has a very important effect on pore size of CA. Also, more variability of results was observed within the two samples activated with acid reagent (i.e., CA10A

and CA60A) than within those activated with alkaline reagent (i.e., CA10B and CA60B) which may be considered as an indirect indication of more effectiveness for the alkaline reagent.

Surface chemistry

PZC, functional groups, and acidic or basic groups on the surface CA allows to determine the affinities of the adsorbent towards the component of interest, which in the case of this study is VCA. Additionally, surface chemistry provides information on the influence of electrostatic forces on the adsorption phenomena. For the CA synthesized in this study, the obtained pH_{pzc} were 5.9, 3.8, 9.1 and 6.9 for samples CA10A, CA60A, CA10B, and CA60B respectively. As expected the higher the phosphoric acid concentration during activation, the lower the pH_{pzc} ; however, contrary to expectations [6], the higher the potassium hydroxide concentration during activation, the lower the pH_{pzc} . This may be explained because according to the results shown in Table 1 the mesopore volume of CA60B is greater than that of CA10B. Because of this feature, CA60B may be washed more effectively, thus retention of the activating agent in CA10B is more likely to occur, which results in a higher pH_{pzc} .

Table 1: Pore volumes and surface areas for all AC samples

Sample	V_{total} ($cm^3.g^{-1}$)	V_{micro} ($cm^3.g^{-1}$)	V_{meso} ($cm^3.g^{-1}$)	S_{ext} ($m^2.g^{-1}$)	S_{micro} ($m^2.g^{-1}$)	S_{meso} ($m^2.g^{-1}$)
CA10A	0.254	0.212	0.042	490	474	16
CA60A	0.173	0.132	0.041	280	265	15
CA10B	0.345	0.275	0.065	810	784	26
CA60B	0.367	0.289	0.078	772	705	67

**Table 2. Functional groups obtained by Boehm titration
Concentration in mmol of functional group/g CA**

	pH_{pzc}	CG	LG	PG	BG
CA10A	5.98	1.69	0.060	0.080	2.95
CA60A	3.80	1.71	0.040	0.060	2.90
CA10B	9.07	1.67	0.005	0.028	2.67
CA60B	6.09	1.60	0.050	0.040	3.10

CG: carboxylic groups

PG: phenolic groups

LG: lactonic groups

BG: basic groups

Boehm titrations were performed for the four CA samples; the results are shown on Table 2. Given the complexity of the superficial chemistry of carbonaceous materials, the characterization and quantification of the different functional groups on the surface is not straightforward.

Carboxylic groups (CG) were very similar for all samples; however, sample CA60A, showed a CG content slightly higher than that observed for all other samples. This result correlates well with the lowest pH_{pzc} also observed for the CA60A sample. Interestingly, the sample with the highest pH_{pzc} (CA10B) does not contain the highest basic groups, which rather correspond to CA60B.

Fourier transform infrared spectroscopy (FT-IR)

A notable difference exists in the spectra obtained for the precursor before and after activation. Oil-palm shell and the 4 produced CA contained (C=C) double-bonds. However, after activation (C-O) bonds become present. Formation of oxygen-carbon bonds is the result of the hydration of alkenes. Changes such as this, may become determinant for the affinity of CA to certain compounds during adsorption.

Thermogravimetric Analysis (TGA) and Differential Thermal Analysis (DTA)

Mass losses between 30 and 100°C are attributed to the elimination of water absorbed in the CA pores. Through TGA, it was determined that the CA with the highest mass loss rate in this temperature range was the CA60A, with 14% followed by CA60B with 10%, CA10A with 9% , and CA10B with 7.5%.

In the range of 145 to 575°C no considerable mass loss occurs in any of the 4 samples of CA, but the decomposition of the material continues. All samples showed similar behavior at temperatures lower than this point (Figure 4); nevertheless two tendencies become apparent beyond 580°C, making a clear difference between CA activated with acid reagent (CA10A and CA60A exhibited a 5 to 10% mass loss) and those activated with a basic reagent (the mass loss observed for CA10B and CA60B was close to 1%). These losses are related to thermal decomposition (pyrolysis) of volatile solids still present in the CA samples⁹⁻¹¹. Because of this, it becomes apparent that during carbonization regeneration, carbons CA10B and

Table 3: Adsorption isotherm models used and their parameters¹⁰⁻¹²

Isotherm	Model	Parameters
Langmuir	$q_e = \frac{b q^0 C_e}{1 + b C_e}$	C_e : liquid phase equilibrium concentration (mg/L) q_e : equilibrium adsorption capacity (mg/g) b : Langmuir constant (L/mg) q^0 : maximum adsorption capacity
Freundlich	$q_e = K_F C_e^{1/n}$	K_F : Freundlich constant (L/mg); $1/n$: heterogeneity factor
Templin	$q_e = \frac{K_T}{b_T} \ln(A C_e)$	A : Templin constant (L/g) b_T : Templin constant
Redlich-Peterson	$q_e = \frac{K_R C_e}{1 + a C_e^\beta}$	K_R : Redlich-Peterson constant (L/g) a : constante de Redlich-Peterson (L/mg) β : constante Redlich-Peterson (L/g)
Langmuir-Freundlich	$q_e = \frac{q^0 (K_{LF} C_e)^{a_{LF}}}{1 + (K_{LF} C_e)^{a_{LF}}}$	K_{LF} : Langmuir-Freundlich constant (L/mg) a_{LF} : heterogeneity parameter.

CA60B would be preferable as they result in lower total mass loss at high temperatures.

Adsorption results and effect of adsorbent mass

All carbons adsorbed VCA but those impregnated with KOH showed higher adsorption capacity. Among all, CA60B showed the highest adsorption capacity. It was estimated as 2.64 g of CA60B would be required to achieve almost complete removal of VCA from the solution at 30°C. On the other hand, Figure 5 shows the effect of adsorbent mass on the adsorption process. An increase in acid removal was observed as activated carbon mass was increased. On the contrary, adsorption capacity, expressed as equilibrium adsorbent phase concentration, decreases as carbon mass is increased. This occurs in the case of all four adsorbents studied. Two factors may contribute to this effect: as adsorbent dose increases, adsorption sites remain unsaturated during the adsorption reaction, leading to a decrease in adsorption capacity; or the aggregation and agglomeration of carbon on the test jars leads to less superficial area becoming available and increasing the distance for acid diffusion^{10,11}.

Effect of initial concentration

Figure 6 shows the effect of initial concentration of the solution of carboxylic acids in

which the CA was immersed for the adsorption process to occur. Results are shown for the case of butyric acid, which is the largest VCA of interest in the context of this study. Results evidenced a decrease in acid removal with higher initial concentrations. On the contrary, adsorption capacity increased with initial concentration of acids in the solution.

The effect of initial concentration is similar for the four adsorbents studied. This would indicate that in general the adsorption process is enhanced by a larger concentration of VCA in the stock solution, possibly due to a higher availability of acid molecules resulting in a larger driving force for mass transfer. On the other hand, the reduction of removal percentage could be caused by a descent in adsorption rates due to the saturation of open pores and surface available. Comparing all CA, CA60B showed the highest acid removal.

Equilibrium isotherms and adsorption thermodynamics

Adsorption isotherms qualitatively assess the nature of surface-solute interactions and specific relations between the adsorbate concentration and its accumulation on the surface of the adsorbent at a constant temperature¹⁰⁻¹². In order to study the nature of the adsorption of acetic, propionic and

Table 4: Adsorption isotherm parameters for CA60B

Isotherms	Parameters	30°C	40°C
Langmuir	q_0 (mg/g)	1565.88	1906.96
	b (L/mg)	0.061	0.090
	R^2	0.946	0.987
Freundlich	K_F (L/mg)	119.49	228.05
	N	1.475	
	R^2	0.938	
Tempkin	A (L/g)	1.264	
	b_T	10.80	
	R^2	0.883	
Redlich-Peterson	K_R (L/g)	68.40	
	a (L/mg)	8.35E05	
	λ	3.064	
	R^2	0.952	
	R^2	0.946	
	K_{LF} (L/mg)	0.062	
	a_{LF}	1.006	

butyric acid on four adsorbents (CA10A, CA60A, CA10B y CA60B) five models were used to fit experimental data, Langmuir, Freundlich, Tempkin, Redlich-Peterson and Langmuir-Freundlich. Equations for each model are presented in Table 3. Model parameters were determined by non-linear regression using Minitab16® statistical software

and are presented in Table 4. Figure 7 illustrates the different adsorption isotherm models for CA60B adsorbent at 40°C.

The Langmuir model is usually implemented on the assumption of ideal monolayer adsorption¹⁰ and it is usually used for

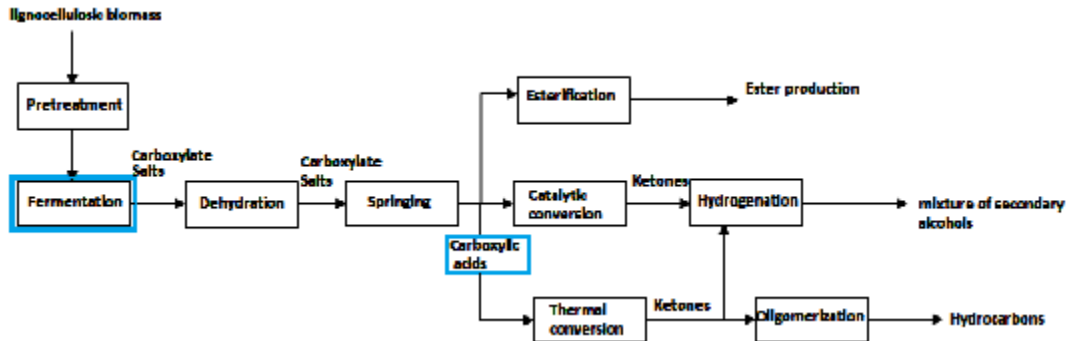


Fig. 1: General scheme of the MixAlco® Process

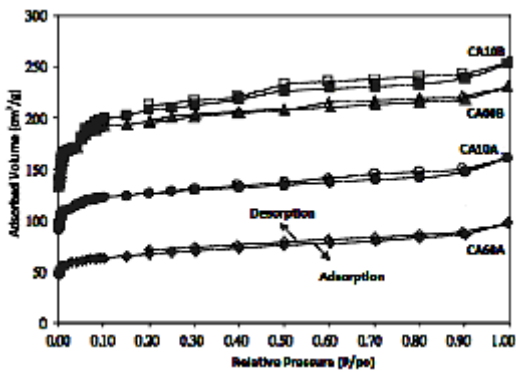


Fig. 2: Nitrogen adsorption isotherms for CA10A, CA60A, CA10B and CA60B

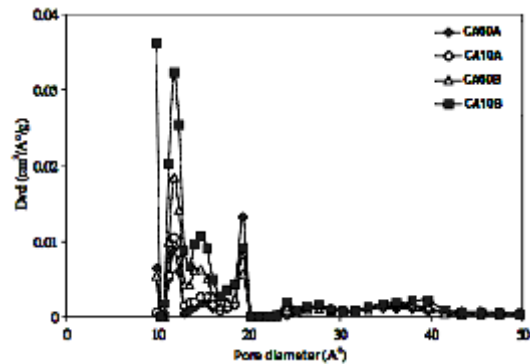


Fig. 3: Pore distribution for CA10A, CA60A, CA10B and CA60B

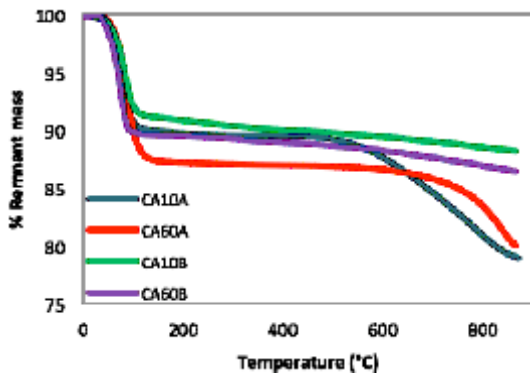


Fig. 4: Thermogravimetric analysis for the carbons CA10A, CA60A, CA10B and CA60B.

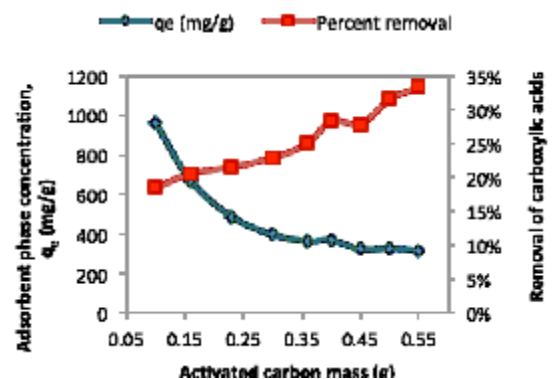


Fig. 5: Effect of adsorbent mass on adsorption of carboxylic acids. CA60B, T=30°C

heterogeneous adsorption surfaces. The Redlich-Peterson model, for its versatility, is applicable to homogeneous and heterogeneous systems over a wide range of concentrations¹²⁻¹⁵. The Freundlich model describes appropriately multilayer adsorption processes with interaction between adsorbed molecules¹³. The Tempkin model is employed to show the effect of some indirect adsorbate-adsorbate interactions¹⁴.

Using the determination coefficient (R^2) as only indicator it was found that the Redlich-Peterson

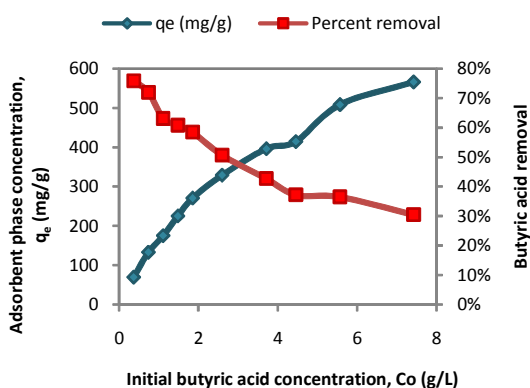


Fig. 6: Effect of initial concentration on adsorption of butyric acid. CA60B, $T=40^\circ\text{C}$

model presented the best fit for the experimental data. This evidences the versatility of the Redlich-Peterson model. However, this model is highly affected by experimental variability. This makes it not the best alternative to predict the behavior of the adsorbents.

The Langmuir-Freundlich model was found to be the best representation of experimental equilibrium data for the four carbons used at both temperatures. This suggests that the surface of the four adsorbents might be heterogeneous with

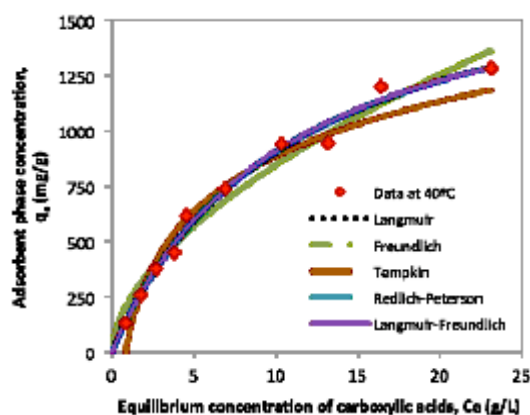


Fig. 7: Comparison of different isotherm models for adsorption of carboxylic acids on CA60B at $T=40^\circ\text{C}$. C_e : liquid phase equilibrium concentration (mg/L) and q_e : equilibrium adsorption capacity (mg/g)

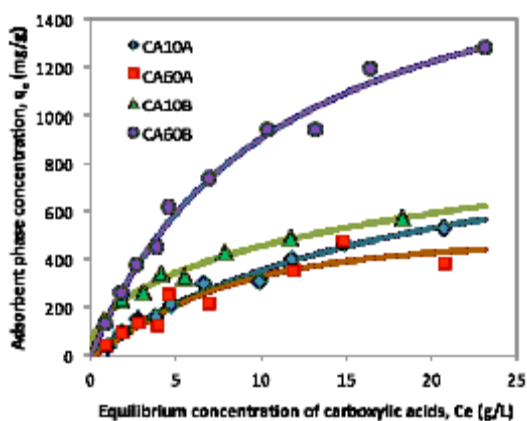


Fig. 8: Comparison of activated carbons on the adsorption of carboxylic acids. $T=40^\circ\text{C}$. Fitted to Langmuir-Freundlich model. C_e : liquid phase equilibrium concentration (mg/L) and q_e : equilibrium adsorption capacity (mg/g)

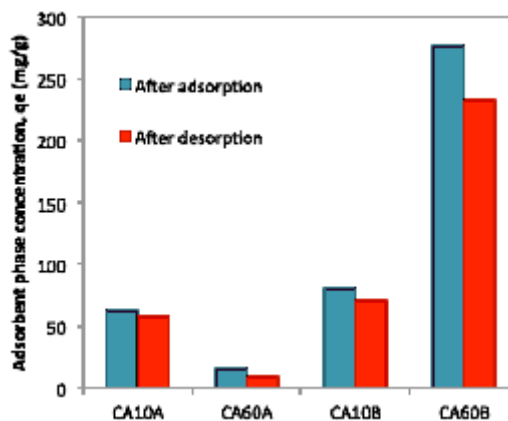


Fig. 9: Adsorbent phase concentration comparison after adsorption and after desorption. q_e : equilibrium adsorption capacity (mg/g)

different energy distributions^{14,15}. Additionally, as Langmuir model has a better fit than Freundlich model, it is inferred that in most cases adsorption occurred in monolayer (as opposed to the multilayer scenario)¹⁰, with the exception of CA10B. The value of the determination coefficient for the models using CA10B shows a change in goodness of fit with temperature, where at 30°C Langmuir model presents a better fit than the Freundlich model. The opposite occurs at 40°C.

Adsorbent comparison

Figure 8 compares the adsorption capacities of the four adsorbents studied at 40°C. A similarity is observed between carbons activated in acid medium, both of which showed the lowest adsorption capacities. The adsorption capacity of CA10A is slightly higher than that of CA60A. This might happen due to a less favorable superficial chemistry for adsorption of carboxylic acids when activation occurs in an acid medium. Increasing concentration of the acid impregnation medium for the activation would therefore decrease adsorption capacity of short chain carboxylic acids. Carbons activated in a basic impregnation medium have higher adsorption capacities. CA60B presents the highest adsorption capacity, well above the other carbons.

Experimentally, it was found that changing temperature, initial acid concentration and adsorbent mass causes changes in adsorption capacities and carboxylic acid removal percentage. These experiments had in common CA60B as a dominating adsorbent for the recovery of carboxylic acids. Higher adsorption capacity for CA60B could be caused by a higher development in porosity and a more favorable superficial chemistry.

Desorption

The results of the desorption study are shown in Figure 9. Because all measurements were taken after 24 h of samples in either adsorption or desorption conditions, the equilibrium was reached, which guarantees that no more VCA were to be adsorbed or desorbed from the CA surfaces. The percentage of desorbed acids from the CA surface were 7.5%, 41%, 12%, and 16% corresponding to CA10A, CA60A, CA10B, and CA60B respectively. This is a low percentage that forces to reconsider

either the use of CA as synthesized in this study as a recovery mechanism for carboxylic acids in the MixAlco® process, and/or the desorption mechanism proposed here.

Adsorption of short chain carboxylic acids from aqueous solutions on activated carbon is ruled by two main interactions: physical and chemical¹³⁻¹⁷. Physical interactions are mainly dispersive interactions, including the effect of microporosity, and specific hydrogen bonds. Chemical interactions include the effects of surface chemistry such as acid-base interactions. Because of these interactions, the surface of basic carbons such as CA60B, allows acid-base reactions, generating a higher presence of acids on the surface of the carbon. Additionally the high porosity of CA60B favors both adsorption and desorption processes.

CONCLUSIONS

It was possible to properly synthesize CA from oil palm kernel shells using both acidic (A) and alkaline (B) reagents at two very different concentrations (10 and 60% w/w). All 4 samples of obtained carbon, i.e., CA10A, CA60A, CA10B, and CA60B significantly increased their surface area and pore volume during activation of fixed carbon in the shells. After characterization it was found that CA10A and CA60A present an acidic surface with pore diameter between 1 and 4.2 nm, while CA10B y CA60B present a basic surface with pore diameter between 0.96-5nm. From all CAs obtained in this study, CA60B evidenced the greatest adsorption capacity reaching 1300 mg of adsorbed acids/g of carbon, corresponding to 33.3% of acids present in the solution.

Langmuir-Freundlich model describes more appropriately the adsorption phenomena observed for all four adsorbents. The four carbons present a heterogeneous surface. Desorption proved difficult during temperature shift studies using warm water. Difficulty in recovery of surface adsorbed acids make CA as produced in this study a poor choice for the fermentation stage in the MixAlco® process. To improve desorption, activated carbons should be synthesized with higher mesopore volume and/or other desorption mechanism should be assessed.

ACKNOWLEDGEMENTS

The authors wish to thank the Master Agreement established between the 'Universidad

de los Andes' and the 'Universidad Nacional de Colombia' and the Memorandum of Understanding entered into by the Departments of Chemistry of both Universities.

REFERENCES

1. Chazdon, R.L. *Science*. **2008**, *32*, 1458-1460.
2. Holtzapple, MT; Davison, RR; Ross, MK; Aldrett-Lee, S; Nagwani, M; Lee, CM; Lee, C; Adelson, S; Kaar, W; Gaskin, D; Shirage, H; Chang, NS; Chang, VS; Loescher, M.E., *Appl. Bio.B.* **2013**, *77*, 609-631.
3. Nachiappana, B.; Fu, Z.; Holtzapple, M.T. *Bioresource Technology*, **2011**, *102* (5), 4210-421.
4. Zhihong, F.A.; Holtzapple, M.T. *Bioresour. Technol.* **2009**, *101*, 2825-2836.
5. Dias, J.; Alvim, M.; Almeida, M.; Utrilla, J.; Polo, M. *J. Environ. Manage.* **2007**, *85*, 833-846.
6. Boehm, H.P. *Carbon* **1994**, *32*, 759-764.
7. Ania, M.C. Purification of Industrial Effluents with Activated Carbon, Adsorption of Pollutants and Adsorbent Regeneration. Doctoral Thesis, Universidad de Oviedo. Asturias (Spain), 2003.
8. International Union of Pure And Applied Chemistry. Reporting physisorption data for gas/solid systems with special reference to the determination of surface area and porosity. Great Britain, **1982**, *54*, 2201-2218.
9. Sing, K. S.; Haul, R. A.; Pierotti, R. A.; Siemieniowska, T. *Pure & Appl. Chem.*, **1985**, *57*(4), 603-619.
10. Giraldo, L.; Ladino, Y.; Moreno-Piraján, J.C.; Rodriguez, M.P. *Eclet. Quími.* **2009**, *32*, 55-62.
11. Li, K.; Zheng, Z.; Xingfu, H.; Zhao, G.; Feng, J.; Zhang, J. *J. Hazard. Mater.* **2009**, *166*, 213-220.
12. Langmuir, I. *J. Am. Chem. Soc.* **1918**, *40*, 1361-1403.
13. Foo, K.Y. *Chem. Eng. J.* **2010**, *168*, 2-10.
14. Derylo-Marczewska, A.; Jaroniec, M.; Gelbin, D.; Seidel, A. *Chemica Scripta.* **1984**, *24*, 239-246.
15. El-Sayed, Y.; Bandosz, T. *J. Colloid Interface Sci.* **2004**, *273*, 64-72.
16. Li, Y.H.; Zechao, D.; Jun, D.; Dehai, W.; Zhaokun, L.; Yanquin, Z. *Water Res.* **2005**, *39*, 605-609.
17. Zelentsov, V.; Datsko, T.; Dvornikova, E. Adsorption model for treatment of experimental data on removal fluorine from water by oxihydroxides of aluminium. *Romai. J.*, **2012**, *8*, 209-2015.